How does pressure effect the plasma breakdown voltage of air as a fuel source in the designed IEC fusion reactor?

<u>Table of Contents</u>

Introduction

Regarding that a whopping 67% of the electricity share by fuel type of the World's energy production comes from burning fossil fuels (figure 1), unsustainable sources that are being depleted faster than ever as a result of increased demand worldwide with the release of greenhouse and flue gasses, it is no surprise to see the devastating environmental consequences and the creation of an alarming situation that needs our dire attention. As a result, renewable energy production responses such as solar, wind, hydro and bio-energy gained "popularity", however, they can be unreliable and unevenly distributed. As a response, other alternatives such as nuclear fusion was considered.

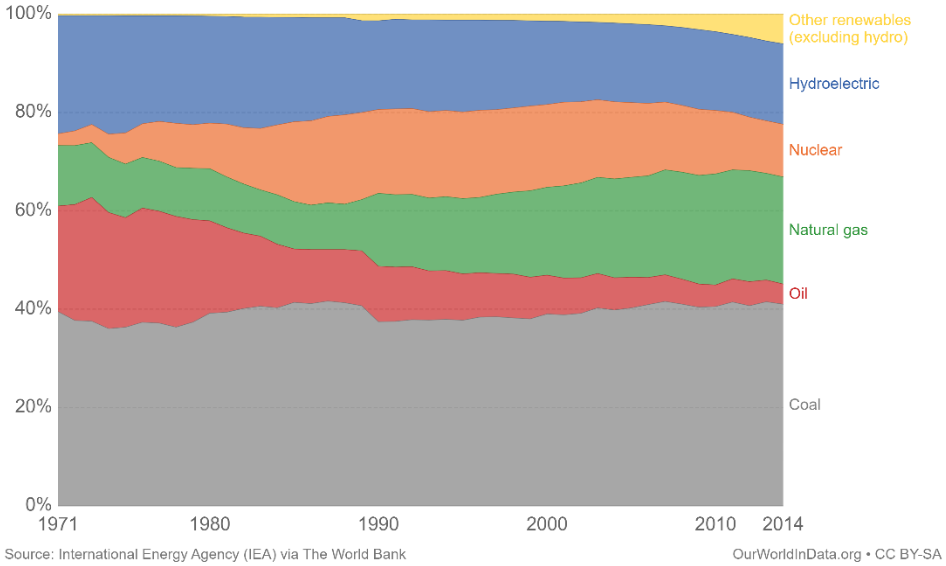

Figure 1: Worldwide electricity share by fuel type (University of Oxford, n.d.).

Nuclear Fusion, unlike Nuclear Fission, is a clean and a sustainable energy source. With its most common fuels (isotopes of hydrogen; *Deuterium* ${}^{2}_{1}H$ and *Tritium* ${}^{3}_{1}H$), being abundantly available and easy to synthesize, without long-lived radioactive wastes and characteristically safe reactors with no possibility of a meltdown deems this technology to have the potential to power our cities in the future.

In this study, I will be exploring the potential of this technology by designing, modelling and building my own Inertial Electrostatic Confinement Fusion Reactor (SIEC-K). Furthermore, I will be examining how the pressure value in the reactor effect the plasma breakdown voltage. The pressure will be altered using a vacuum pump and a manometer. The voltage will be monitored using a high voltage probe connected to a voltmeter. The plasma will be observed using the viewport installed in the reactor. The obligatory safety standards under a legal manner are met by the initiative of the supervisor delegated from National Atomic Energy Authority. These include but are not limited to; maintaining safety during the operation of the reactor, general safety of the personnel and high voltage operation safety certificate. The reactor will only be operated in glow-discharge plasma (studying the plasma ignition conditions) and no nuclear reactions will be formed, thus, there will be no radiation risks involved. All applications regarding the usage of the reactor will be conducted by the assistance of the attendant physics teacher and technicians authorized to use high voltage power supplies. The reactor is housed in a university laboratory for further safe keeping.

Background Information

Fusion Basics

The challenge to produce Nuclear Fusion reactions is to overcome the coulomb barrier, the repulsion force between two positively charged nuclei, in order for the reactants to come close enough for the quantum tunneling affect to take place. When this occurs, the fuels inside the reactor collide, fusing and releasing resultant particles and energy. In order to overcome the coulomb barrier, particles must gain a considerable amount of kinetic energy. The most common ways to reach this energy criteria is through thermonuclear fusion, which is achieved by heating the fuel into a plasma and confining it. There are two preferred methods to approach this: magnetic confinement where a magnetic source is used to both confine and heat the plasma and inertial confinement where a source of X-ray is introduced to the fuel pallet at the center of the reactor for it to "implode" in high pressure and temperature, confined by its own inertia. Both of these methods require highly sophisticated machinery and engineering, a deep understanding of complex models involved in nuclear and plasma physics, with generous funding at one's disposal. For the sake of feasibility to achieve a cost-effective reactor, other methods must be considered. Mainly a source of hope when it comes to practicality is Inertial Electrostatic Confinement (IEC) approach which traps ions using an electric field under vacuum with a controlled amount of gas to produce fusion reactions. This technology will be elaborated further to explain its benefits and cons.

$$ {}_{1}^{2}D + {}_{1}^{2}D \rightarrow {}_{1}^{3}T\ (1.01\ MeV) + p(3.02\ MeV)\ [50\%] $$

$$ {}_{1}^{2}D + {}_{1}^{2}D \rightarrow {}_{2}^{3}He\ (3.82\ MeV) + {}_{0}^{1}n(2.45\ MeV)\ [50\%] $$

Figure 2: Possible reactions between D-D fuel (European Nuclear Society, n.d.).

Inertial Electrostatic Confinement Fusion Reactors

An inertial electrostatic confinement fusion reactor (IEC Fusor) is a device that confines the fuel (primarily deuterium gas) by ionizing the gas inside an electrostatic field. It consists of two aligned spherical electrodes where the potential difference is applied such that the inner electrode becomes negatively charged and the outer electrode is grounded (Figure 3). The positively charged ionized particles inside the field moves towards the center through the partially transparent cathode. As the ions move through the center due to the difference in charge in electrodes, they will gain a significant amount of energy capable of undergoing fusion reactions as their density increases. Ideally in a perfectly symmetrical geometry, the ions will always accelerate aiming for the center of the reactor, where high density and energy ions are created, thus increasing the probability of fusion reactions taking place proportionally. As this situation is not feasible due to unideal engineering complications, the ions that are not perfectly accelerated through the center do not fuse and deaccelerate towards the outer space and just before they hit the anode, they turn around to repeat the cycle. As a result they are confined by their own inertia, showing an oscillatory motion between the anode and cathode until the nuclei fuse.

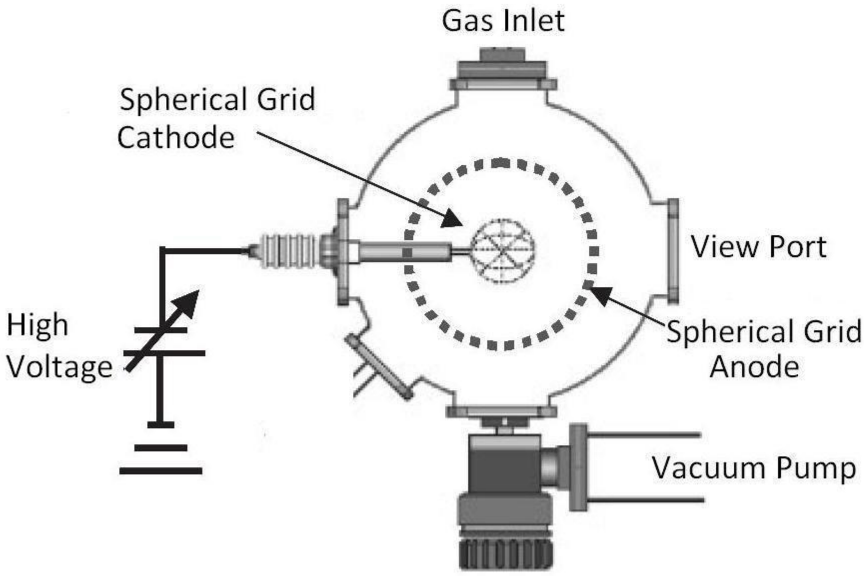

Figure 3: Simple IEC reactor design (Hermans, 2013).

In this study as aforementioned, nuclear reaction will not be performed due to safety restrictions, therefore, the system will be used as a plasma reactor and fusion cross-sections and mechanisms will not be examined. The study will include plasma breakdown voltage calculations using Paschen's Rule and relevant experiments regarding the plasma breakdown voltage depending on the change in pressure, electrostatic modelling of the reactor and experimental analysis.

Paschen's Law

In order for plasma to occur in the reactor, a certain level of ionization is required. To ionize gases, an electrostatic approach can be used where a certain amount of electrical potential is applied between two sources where gas is present. In IEC reactor models, deep potential well in the center of the reactor is where the negative potential is maximum, therefore, the plasma is expected to be observed there. To calculate the plasma breakdown voltage, Paschen's law is used (Wagenaars, 2006):

$$V_b = \frac{Bpd}{\ln(pd) + k}$$

Where k is:

$$k = ln\left[A/\ln(1 + \frac{1}{\gamma})\right]$$

Where p (Torr) is the pressure, d (cm) is the distance between electrodes , γ is the second ionization coefficient, A *($cm^{-1}Torr^{-1}$)* (saturation ionization at a particular electric stress/pressure) and B *($cm^{-1}Torr^{-1}$)* (excitation and ionization energies) are constants relevant to the type of gas (Martins A. a., 2011).

Since this study will mainly focus on the operation of the reactor without producing nuclear reactions, air is determined to be the most suitable fuel. Experimental values for constants in Paschen's law for air is given in table 1.

Constant	Value
γ	*0.01*
A	*15 ($cm^{-1}Torr^{-1}$)*
B	*365 ($cm^{-1}Torr^{-1}$)*

Table 1: Constants for air (Wagenaars, 2006).

Paschen's law is applicable in systems where electrodes are parallel. Obviously, IEC setups are comprised of spherical electrodes, however, the principle is the same (van Limpt, 2013).

To better visualize the parameters within the equation, the graph of this function is given (graph 1).

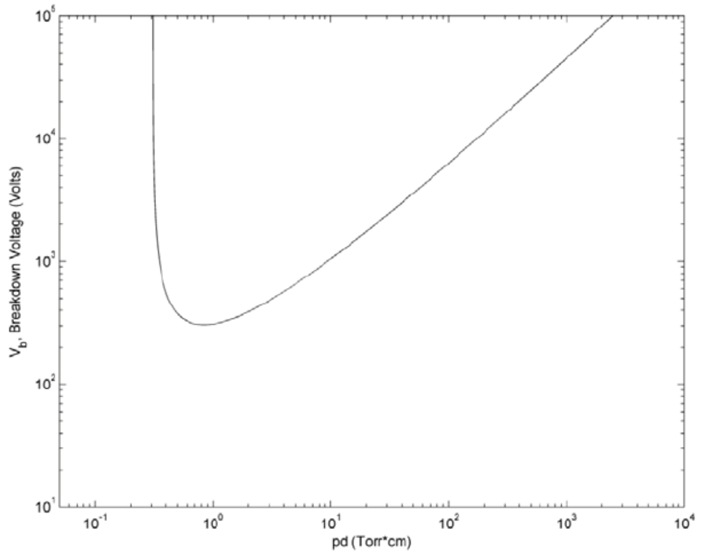

Graph 1: Paschen's curve for air (Voltage versus pressure times distance) (Martins & Pinherio, 2011).

As it can be seen from the graph, the breakdown voltage depends on distance between electrodes, pressure and the type of gas. Potential and electric field in the system are not uniform and inversely proportional to the distance. To better understand the electrostatic properties of spherical IEC fusors, electrostatic modelling will be made.

Electrostatics

The IEC fusors consist of two concentric electrodes, where anode (outside) serves as a vacuum chamber and is kept grounded and cathode is kept at a negative voltage. Under operation, due to the electrostatic potential in the reactor, electrons are attracted to the anode and ions are pulled towards the cathode, which is the center of the reactor. The equations in spherical systems are given.

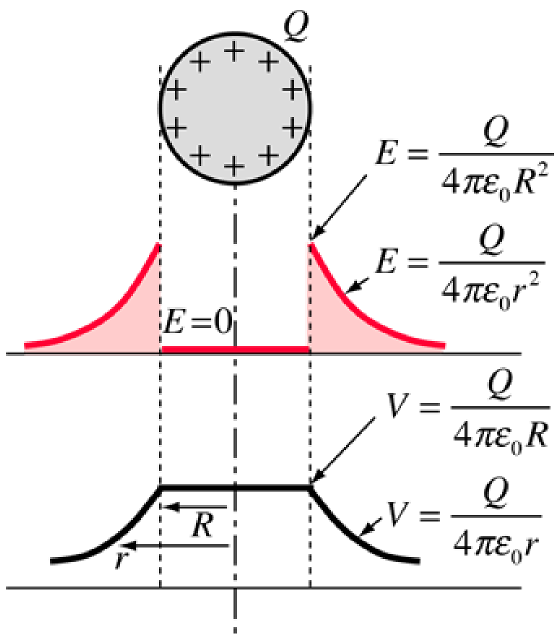

Equation 1: Electric field and potential in spherical geometry (HyperPhysics, 2000).

Given equations for electric field and potential for spherical geometry are valid for calculations using IEC geometry however, doing them by hand in every point in the reactor would be challenging, therefore, 2D electrostatic modelling of the reactor will be made using Quickfield Student Edition simulation program.

Research Question

How does pressure effect the plasma breakdown voltage of air as a fuel source in the designed IEC fusion reactor?

Hypothesis

The plasma breakdown voltage depends on pressure and potential in the system. As pressure increases, the amount of gas that needs to be ionized increases accordingly. This suggests that at only when higher potential levels are applied, where the potential hill's strength is increased, the fuel can ionize and the plasma can be seen.

Simulation Efforts

The electrostatic simulation will be made to see if the reactor model can produce a potential well in the center where ions are supposed to be trapped. Parameters that will be used in the Quickfield 2D electrostatic simulation software are given in table 2 (The specifications used regarding the reactor electrodes and power supply will be elaborated on the experimental setup section).

Simulation Inputs	Anode	Cathode
Outside Diameter	25.5 cm	5 cm
Potential	0 Volt	8000 Volt
Electric Permittivity	8.8542e-12 F/m	8.8542e-12 F/m

Table 2: Simulation inputs.

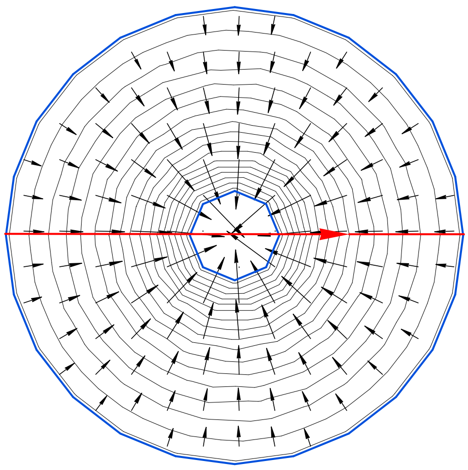

Figure 4: Ion displacement vectors (in black) and contour (in red) where the potential values inside the reactor depending on distance is simulated upon.

Length Inside the Reactor (cm)	Potential (V) (±0.001V)
0	0
1.28012	-334.322
2.56024	-685.915
3.84035	-1108.04
5.12047	-1591.4
6.40059	-2147.78
7.68071	-2827.91
8.96083	-3764.69
10.2368	-4918.51
11.5211	-5000
12.8012	-5000
14.0813	-5000
15.3614	-4923.43
16.6415	-3766.51
17.9217	-2828.96
19.2018	-2149.08
20.4819	-1591.77
21.762	-1108.47
23.0421	-686.471
24.3222	-334.95
25.5	0

Table 3: Simulation outputs (distance versus potential).

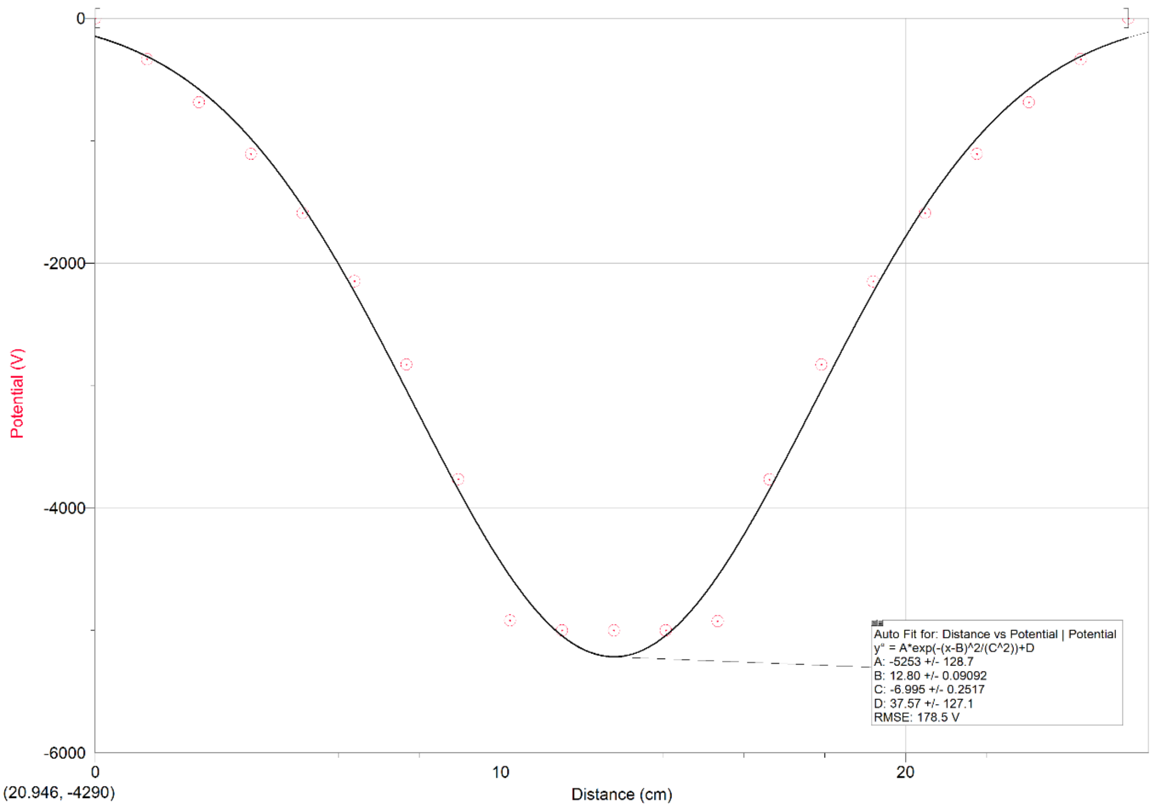

Graph 2: Distance versus potential graph.

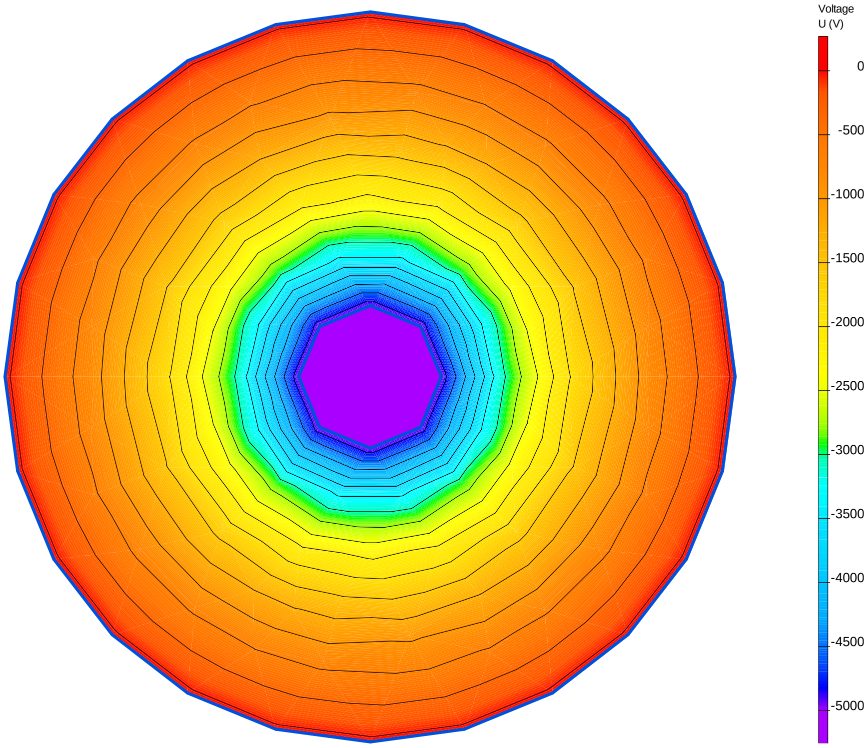

Figure 5: Electrostatic simulation of the reactor model.

As it can be seen from the graph 2 and figure 5, the potential increases towards the cathode, creating a deep negative potential well. Inside the cathode grid it reaches its constant peak level, where the ions will be confined. From these observations, the reactor design is capable of creating a confinement zone, where the plasma is expected to occur. Next step is to design the reactor and build the experiment system to study plasma breakdown.

<u>Experimental Variables</u>

Independent Variable

- Pressure

The plasma breakdown, main study element of this experiment, highly depends on the pressure of the system as indicated by the Paschen's Law. It is directly associated with the amount of fuel inside the reactor that needs to be ionized. To control the pressure, a vacuum system will be installed. The system will be compromised of a rouging pump, which will be used to create the vacuum, a digital monometer (pirani gauge) to measure the pressure inside the reactor in real time and the anode electrode will also be the vacuum chamber.

Dependent Variables

- Plasma breakdown voltage

The plasma breakdown will be observed from the viewport in the reactor. A high resolution camera will be installed to the viewport that will cover all junctions. The feedback will be monitored and recorded from a safe distance and all connections concerning the operation of the reactor will be handled from there.

Controlled Variables

- Sizes and geometry of cathode and anode electrodes

The sizes and geometry of the electrodes can affect the length between them, which will create a different parameter that needs to be considered. This will alter the readings gathered from this experiment so they are kept as constant.

- Type of fuel

Plasma breakdown voltage and pressure differs from the type of gas used in the system. To make a comparison of the findings of this experiment to literature values, the gas used (air) is kept constant throughout the experiment.

- Temperature of the laboratory

Temperature can affect the voltage required to ionize the gas, which will increase uncertainty in the experiment. The laboratory, fuel and initial temperature of the reactor is kept at 25 C degrees.

Procedure and Steps of the Experiment

Material List and Measurement Devices

- 7000 volt DC power supply with installed variac
- High voltage cables
- 55 kΩ resistor
- Main power switch
- High voltage probe
- Multimeter
- Oscilloscope
- High voltage feedthrough
- Reactor Chamber (Anode Electrode)
- Cathode
- Teflon insulator probe
- Acrylic Viewport
- High resolution camera
- Monitor
- Needle Valve
- Monometer (Pirani Gauge)
- Vacuum Pump
- Gas pipe
- Gloves
- Protective Suit
- Acetone and Fiber Cloth

Setup

The purpose of this setup is to make a IEC nuclear fusion reactor and study plasma ignition characteristics of it. To create this, the reactor itself must be designed and other components should be decided and added. The reactor system is comprised of five sections.

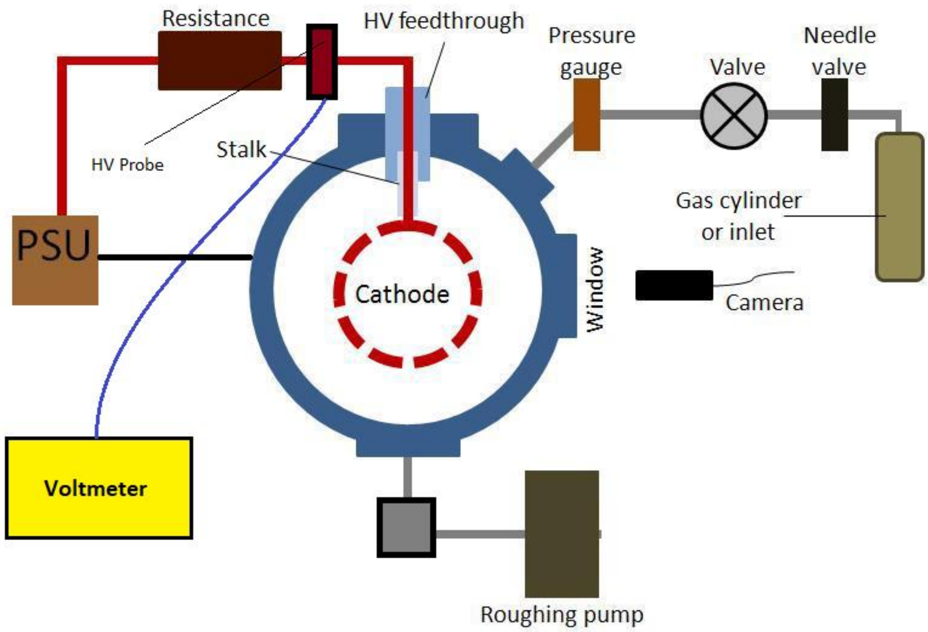

Figure 6: Reactor experiment system setup (edited) (van Limpt, 2013).

1. Chamber System

The reactor chamber will have a spherical geometry. Necessary inputs in the chamber are for vacuum pump, high voltage cathode feedthrough, vacuum gauge, viewport and fuel

First, a draft is drawn to lay out necessary inputs and then, 3D design of it is made. Total of 10 drafts are made and in each of them, the reactor system is optimized and compared to the literature in terms of its cost and functionality. The last design (R10) is actually built and the specifications of it are given.

Design R10 (Diameter 25.5 cm)	**α Angle (degree)**	**β Angle (degree)**	**Length of the Feedthrough**	**Type of Flange**	**Function**
(I)	0	0	9 cm	KF40	HV Feedthrough
(ii)	0	50	3,4 cm	DN50CF	Viewport
(iii)	315	45	3,2 cm	KF25	Vacuum Gauge Inlet
(iv)	45	40	3,2 cm	KF25	Fuel Inlet
(v)	0	180	5,3 cm	DN16CF	Vacuum Pump Inlet

Table 4: Parameters of the reactor design where the alpha angle is for x-axis and the beta angle is for the y-axis.

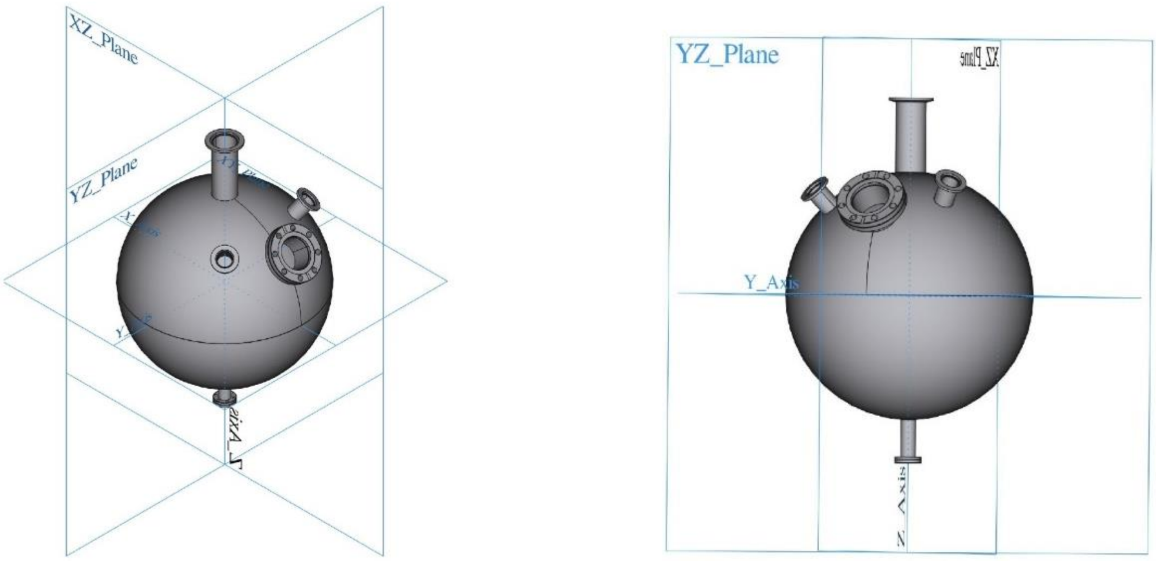

Figure 7: The 3D design of the reactor (axial and frontal views).

The chamber is manufactured from two aluminum blocks which are processed by a CNC machine from given dimensions specified in design R10. The inlets and feedthroughs are TIG welded to the reactor. Finally, all components are connected to the reactor chamber.

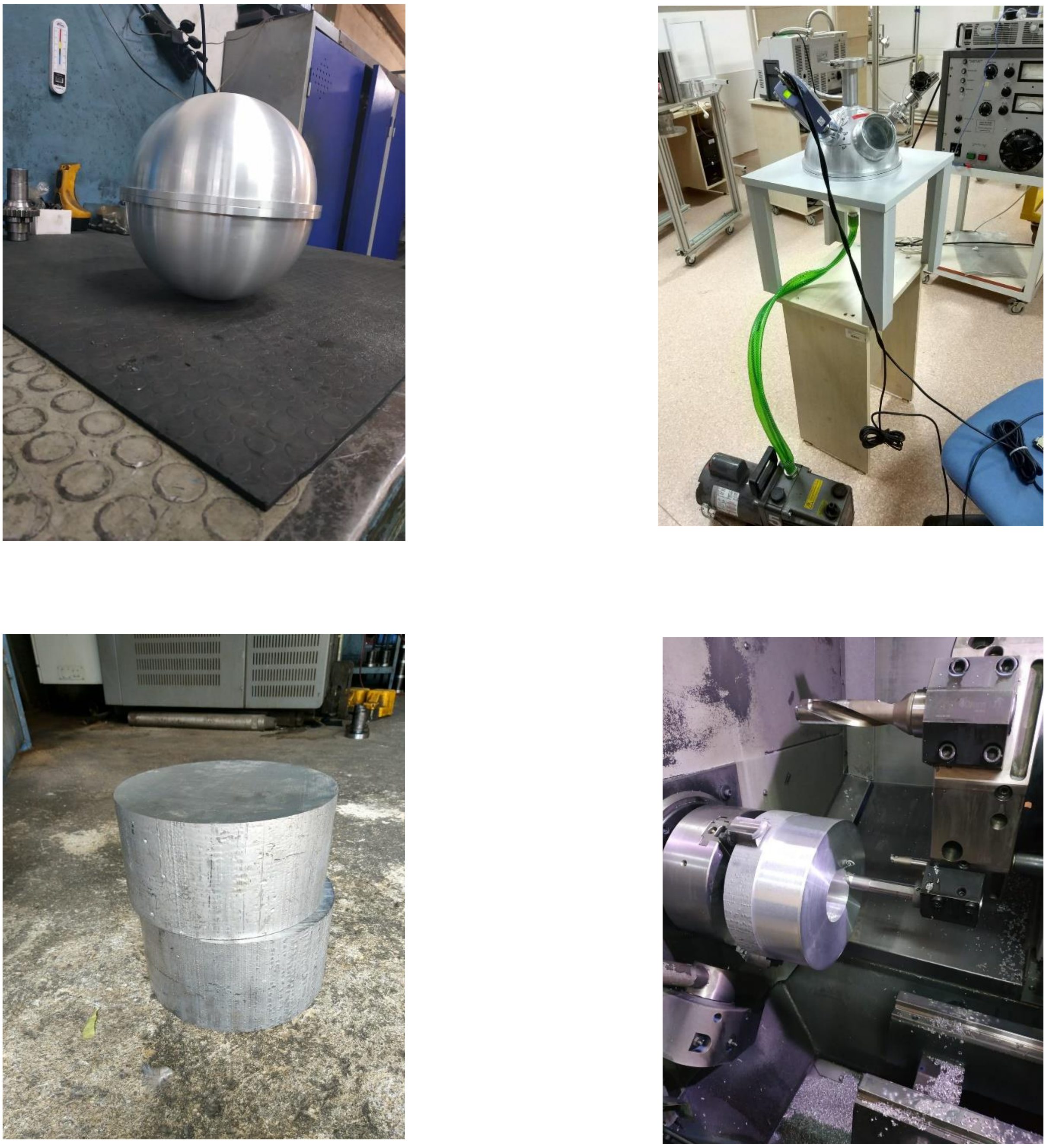

Figure 8: The process of manufacturing and building the reactor chamber

2. Vacuum System

The vacuum system has a roughing pump capable of reaching 10^{-2}-10^{-3} milibar. This is assumed to be enough for conducting plasma studies and control the pressure inside the reactor system. The vacuum pump is connected to the reactor chamber via gas tube that was purchased according to the inlets of the both apparatus.

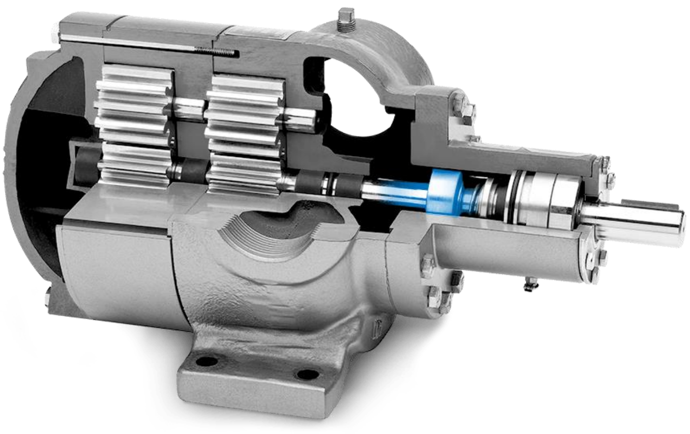

Figure 9: Mechanical roughing pump where the inner system is visible (Smith Pumps, 2019).

3. Power System

The power system have a 7000 Volt DC power supply connected to a 55 kΩ resistor in series to limit the current. This is important considering glow-discharge plasma is expected to be studied in the reactor as it illustrates the fuel's confinement and this phase requires low current values. The phases of plasma in current-voltage values are given in graph 3.

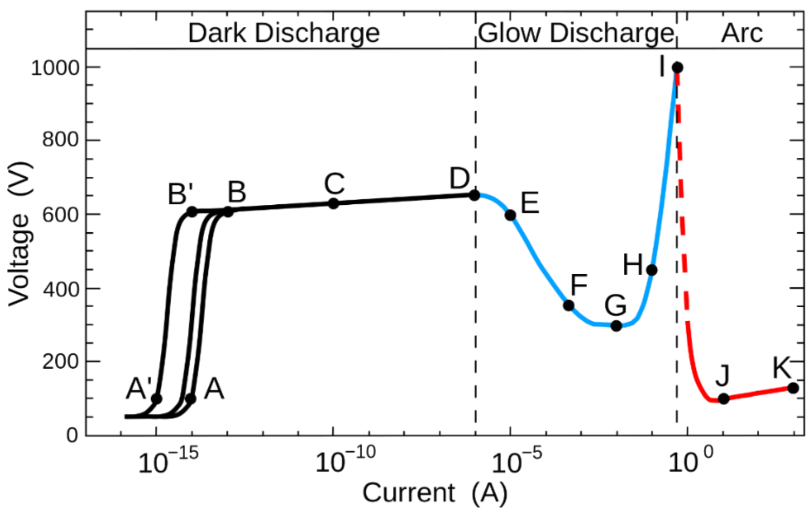

Graph 3: Plasma phase graphic, voltage versus current (Gallo, 1977).

A variac (potential limiter) is connected to the system along with a high voltage voltmeter. The negative terminal is connected to the HV feedthrough that leads to the cathode. Inside the reactor, the part between the spherical cathode grid and feedthrough probe is isolated using a Teflon sheath. This is to protect the reactor from short circuiting and prevent unwanted arcs.

The cathode-anode ratio is around 20%, which is close to the percentage used in other IEC fusion studies (van Limpt, 2013).

Figure 10: The cathode (5 cm. diameter) manufactured from stainless steel.

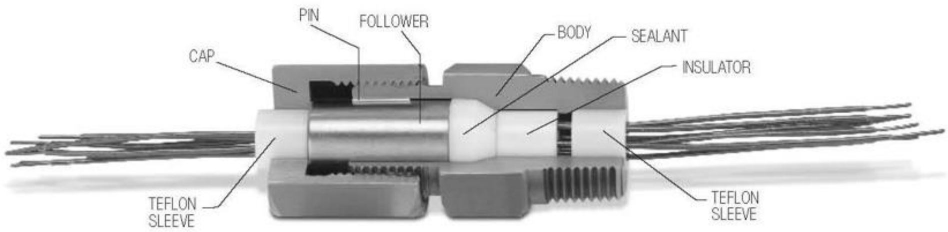

Figure 11: High voltage power feedthrough (Techni Measure, 2016).

4. Fuel System

As the preferred fuel in this experiment is air due to convenience, the only concern is to control the rate of releasement. A needle valve, capable of adjusting the flow rate accurately and slowly, is used for this purpose. The inlet of the gauge will be left open so that it will come in contact to the air inside the laboratory.

Figure 12: Needle Valve (MAKO, 2019).

5. Analysis System

The voltage, pressure and plasma inside the reactor needs to be observed and controlled from a safe distance. To ensure this, all systems coupled to the grid is connected to a main kill switch. The camera, vacuum pump's switch, variac, oscilloscope and multimeter from the voltage probe are placed in a control unit where the operation of the reactor took place.

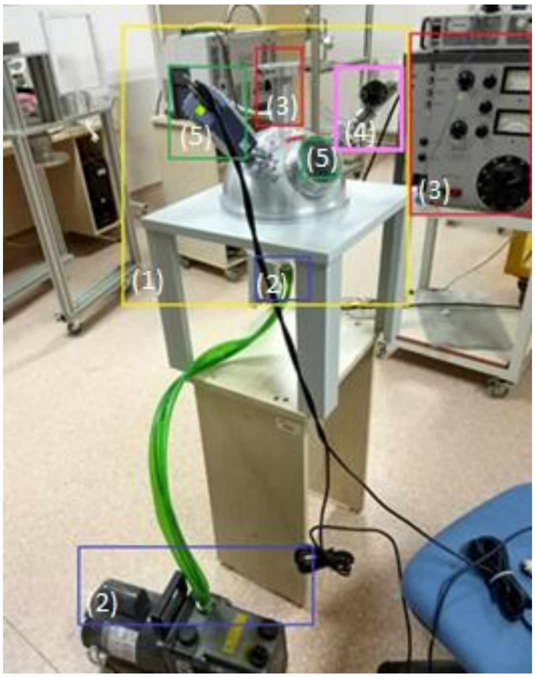

Figure 13: SIEC-K Reactor system

1. Chamber System (Yellow)

2. Vacuum System (Cyan)

3. Power System (Red)

4. Fuel System (Magenta)

5. Analysis System (Green).

Figure 14: The reactor's control system during operation.

Method

- Wipe the inside of the reactor chamber and cathode with acetone to remove particles and contaminations
- Attach the two halves of the chamber and seal it
- Close the needle valve
- Measure the initial pressure inside the reactor
- Turn on the camera and record the real time feed.
- Turn on the vacuum pump and set the pressure to its predetermined value by observing the pressure readout given by the manometer.
- After the pressure value is reached, turn of the vacuum pump, which will seal the reactor (stable pressure in the system is reached).
- Slowly increase the voltage by using the variac installed in the power supply.
- As soon as a spark is observed inside the chamber, record the values for voltage and pressure.
- Repeat this process for every trial and pressure value.

Risk Assessment

The operation of the reactor took place in National University Nuclear Sciences Institute Dosimetry lab where the safety of the personnel and the equipment was strictly monitored by technicians. The reactor did not execute any fusion reactions however, the usage of high voltage power supply and vacuum pump was followed under supervision using a protective suit and gloves. There are no further safety, ethical or environmental considerations to be taken into account.

Data Analysis

Pressure (±0.001 mbar)	Trials	Voltage (±0.1V)	The Lab. Temperature (±0.1 C°)	Size of the Electrodes (±0.1 cm) (Cathode-Anode)	Type of Fuel
2.097	1	864.2	25.0 °C	5.0-25.5 cm	Air
	2	859.2			
	3	861.0			
8.677	1	1799.4	25.0 °C	5.0-25.5 cm	Air
	2	1799.0			
	3	1796.7			
20.000	1	2715.0	25.0 °C	5.0-25.5 cm	Air
	2	2719.5			
	3	2718.6			
28.100	1	3628.0	25.0 °C	5.0-25.5 cm	Air
	2	3623.9			
	3	3620.0			
47.767	1	4570.1	25.0 °C	5.0-25.5 cm	Air
	2	4571.0			
	3	4570.0			
61.700	1	5531.0	25.0 °C	5.0-25.5 cm	Air
	2	5527.5			
	3	5534.2			

Table 5: Data gathered from the relevant experiments.

Uncertainties in the table 5 are determined by the smallest digits the measurement devices have or the given values from their manufacturers.

The data gathered from this experiment is highly dispersed, therefore to analyze it, mean and standard deviation of the groups will be found. Furthermore, the best fit curve will be drawn and then experimental values will be compared to those found using Paschen's law, where it indicates that there is a relation between pressure times distance between the electrodes and the voltage in parallel geometry.

Sample Calculations when Pressure is 2.097 mbar

Calculating Mean

$$Equation\ 2: Mean\ Calculation$$
$$\bar{x} = \frac{\Sigma x}{n}$$
Σx: *The sum of x values*

n: *Number of Data*

$$\frac{864.2 + 859.2 + 861}{3} = 861.5\ V$$

Calculating Standard Deviation

$$Equation\ 3: \text{Standard Deviation}$$
$$\sigma = \sqrt{\frac{\sum(x - \bar{x})^2}{n - 1}}$$
Σx: *The sum of x values*

n: *Number of Data*

$\bar{x}$: *Mean*

σ: *Standard Deviation*

$$V = \sqrt{\frac{(864.2 - 861.5)^2 + (859.2 - 861.5)^2 + (861 - 861.5)^2}{2}} = 2.53\ V$$

Calculating Uncertainty

$$\pm = \frac{Maximum\ Value - Minimum\ Value}{2} \qquad \frac{864.2 - 859.2}{2} = \pm 2.50\ \text{V}$$

Pressure (±0.001 mbar)	2,097	8,677	20,000	28,100	47,767	61,700
Mean Voltage (V)	861,5	1798,4	2717,7	3624,0	4570,4	5530,9
Data Uncertainty	2,50	1,35	2,25	4,00	0,50	3,35
Standard Deviation	2,53	1,46	2,38	4,00	0,55	3,35

Table 6: Data Analysis for values of potential at given voltages.

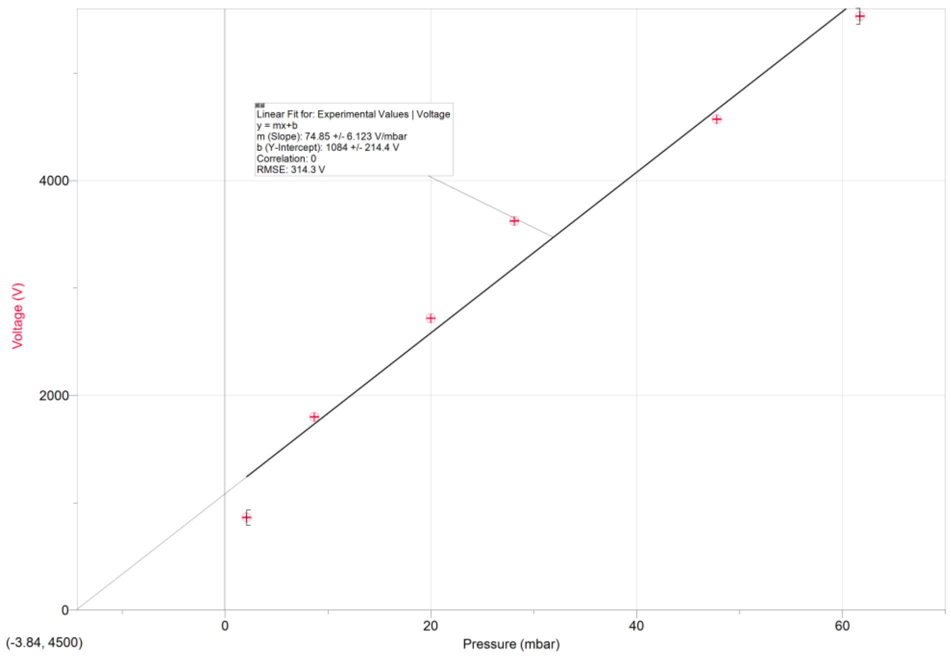

Graph 4: Experimental values of plasma breakdown voltage against pressure. The breakdown voltage increases as pressure increases. Uncertainty values are too low to be seen in the graph.

Calculating Paschen's Values

Constant	Value
γ	*0.01*
A	*15 (cm^{-1}Torr^{-1})*
B	*365 (cm^{-1}Torr^{-1})*

Table 7: Paschen's rule constants for air.

$$V_{breakdown} = \frac{Bpd}{\ln(pd) + ln\left[A/\ln(1+\frac{1}{\gamma})\right]}$$

$$1487.37\ Volts = \frac{365 * 1.57 * 10.25}{\ln(1.57 * 10.25) + ln\left[15/\ln(1+\frac{1}{0.01})\right]}$$

Mean Pressure (±0.001 mbar)	2.10	8.68	20.00	28.10	47.77	61.70
Potential (V)	1487.37	5728.73	11508.50	12032.60	18920.70	23587.00

Table 8: Paschen values of mean pressure and plasma breakdown.

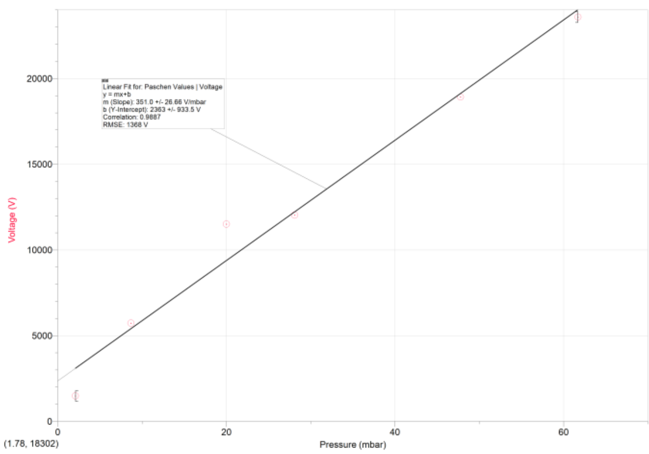

Graph 5: Paschen values of plasma breakdown voltage against pressure. Uncertainty values are too low to be seen in the graph.

Standard deviation show the dispersion of given data, which can be used to test the reliability. If the two standard deviations are smaller than the difference between any means, the hypothesis is supported and the experimental data are reliable (Slichter, n.d.). For all groups, this criteria is satisfied. Relatively high values for standard deviation for the last three groups with potential differences of 3624.0 V, 4570.0 V, 5531.0 V respectively is seen. At these levels of high potential, the gas is observed to ionize quickly at higher pressures. The vacuum pump is fast at pumping the air out of the system and the monometer's digital value output's rate is limited. The pressure changes quickly and at the breakdown voltage, the monometer's readings may be unreliable to a certain degree.

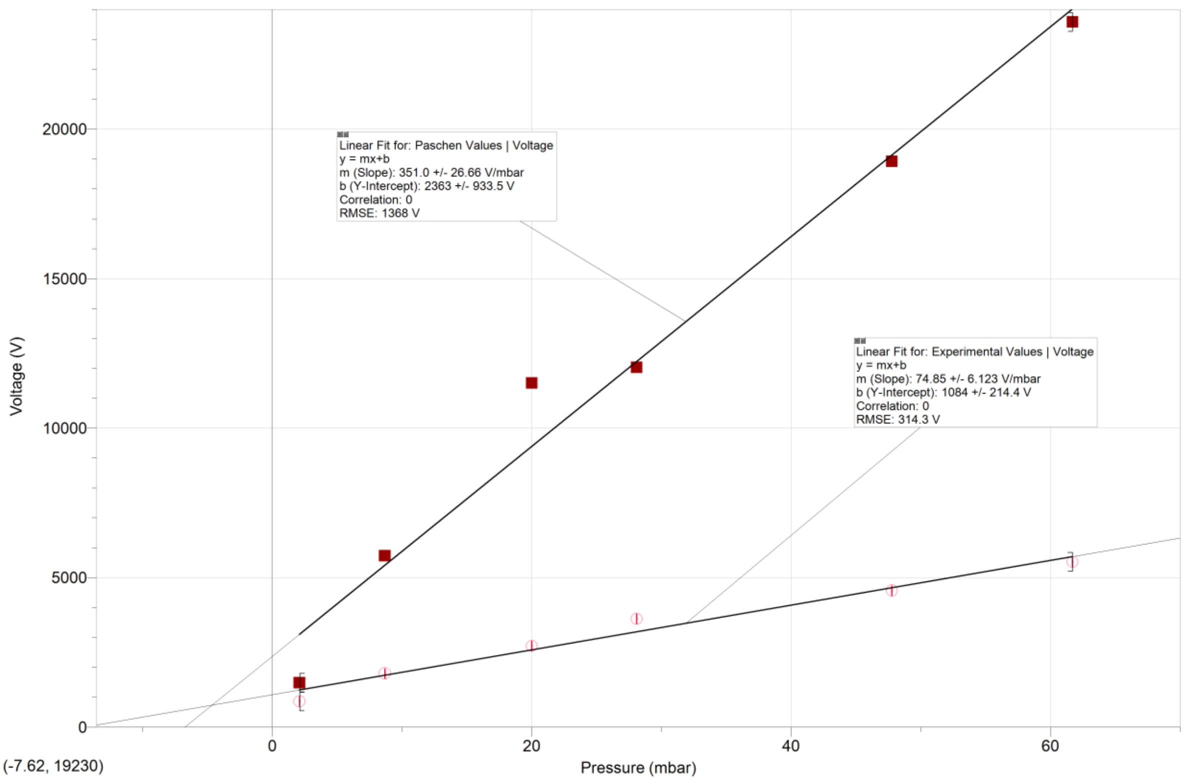

Graph 6: Experimental and calculated Paschen values of plasma breakdown voltage and linear relations of voltage against pressure are shown on the graph.

Percentage Error Calculation:

$\% \text{ Error} = \frac{\Delta \mathrm{m}}{m} \times 100$ $\% \text{ Error} = \frac{6.123}{74.85} \times \mathbf{100} = \mathbf{8.18}\%$

Calculating a Relation between Voltage and Pressure:

Using the slope and y-intercept values extracted from the linear relationship $y = mx + b$ for experimental voltage breakdown values (graph 4), equation below can be found that can apply to the designed reactor SIEC-K.

$$V_b = 74.85p + 1084$$

V_b: Plasma voltage breakdown (V)

p: Pressure (mbar)

<u>Conclusion and Evaluation</u>

The purpose of this study is to analyze the effect of pressure on plasma breakdown voltage using the designed IEC reactor, which in the future, further operations involving nuclear reactions after legal and safety procedures are planned to be made. The operation of the reactor took place in National University Nuclear Sciences Institute dosimeter lab where the safety of the personnel and equipment was closely monitored by technicians. As foreseen, the plasma occurred in the deep potential well at the center of the reactor, confirmed by the simulations (Graph 2) and the breakdown voltage increased exponentially as pressure increased (Graph 5). The figure 16 shows the plasma confined by the deep potential well created by the reactor.

Values for experimental percentage error calculations are extracted from the used graphic drawing program, Logger Pro, using linear fit. 8.18 % of overall error in the experimental values suggests high reliability in the results, especially considering the sensitivity of the apparatus.

Furthermore, comparing Paschen breakdown voltage values with experimental ones would not be valid specific to this study considering the Paschen rule only applies for calculating breakdown voltage for parallel plates. Although Paschen's rule may not be applicable for directing analytical assessment of the experimental values, the fundamental principles stating that the increase in pressure results in the increased breakdown voltage in a curve can be used to make a comparison as suggested in figure 15 and graph 6.

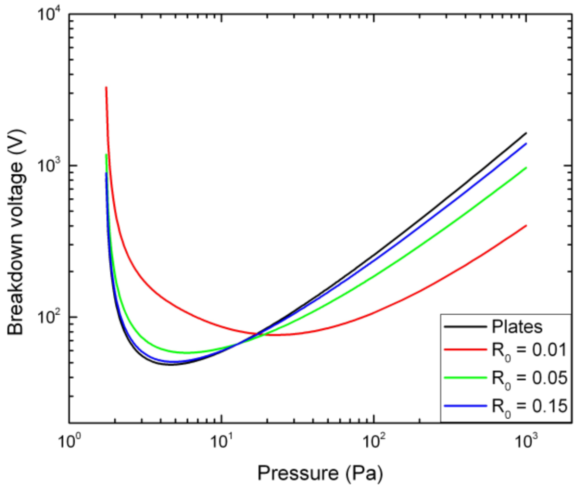

Figure 15: The influence of the spherical geometry on the breakdown voltage. The black line shows the reference curve, the parallel plates Paschen curve. The distance between the electrodes and the secondary electron emission is equal for all lines, 0.1 m and 1.0 respectively (Hermans, 2013).

The experimental values of plasma voltage breakdown showed a linear relation with pressure and an equation for calculation values of breakdown voltage against pressure was found to be $V_b = 74.85p + 1084$. However, as suggested by the figure 15, plasma breakdown voltage against pressure should be a curve regardless of the geometry of the reactor. Reason for obtaining a linear relation is, only a section of the curve was studied considering the potential of the system was limited to 6000 V and pressure was only lowered to 2 mbar due to systematic restraints with both power supply and vacuum pump. Ideally, ranges for both pressure and voltage should be increased to study the full curve. For future systems, this can be implemented but due to a limited budget, it was not a concern for this experiment.

Upon literature examination, no specific equation was found that could have been interpreted by me considering my limited knowledge in plasma physics and calculus. Therefore, the comparison between theoretical and experimental values was not conducted. This is seen in graph 6, as pressure increases, for both Paschen and experimental values, the breakdown voltage also increases with different rates, supported by figure 15.

The experiment system, where the pressure is decreased by using a vacuum while keeping the potential stable, the breakdown values are recorded at the instant when a spark of plasma is seen, as implied by breakdown. The IEC has many plasma characteristics. The main two is the glow-discharge and jet mode. In figure 16, the fusor is working in glow-discharge mode, where the beams of light are emitted from the center of the reactor, caused by the geometry of the grid (Hermans, 2013). The digital output from the monometer, multimeter and video feedback is recorded simultaneously to ensure accuracy. These aforementioned tools for measurement was also calibrated automatically before every experimental trial. After the experiment, how the breakdown voltage is affected by the pressure among other parameters were explored.

Figure 16: The plasma confined in the potential well created in the SIEC-K reactor.

As pressure decreases in the system, the breakdown voltage also decreases as shown in graph 5. This relation is also seen in the Paschen calculations, although the rates differ from the experimental values seen in graph 5. Besides uncertainty during the experiment, the reason for acquiring different values is because of the spherical geometry of the reactor, which allows better central confinement which may be argued for lower breakdown values for IEC setup.

Furthermore, a secondary analysis was made to see the potential change after plasma breakdown (graph 7) to further elaborate on the plasma characteristics of the designed reactor SIEC-K. As the pressure decreases with time, the intensity of the plasma increases, although inconsequential to plasma breakdown. The voltage after the plasma breakdown at 2.1 mbar decreases as the intensity of the plasma increases (Graph 7). As more gas ionizes, the voltage will decrease as some of that potential is lost for the glow of the plasma.

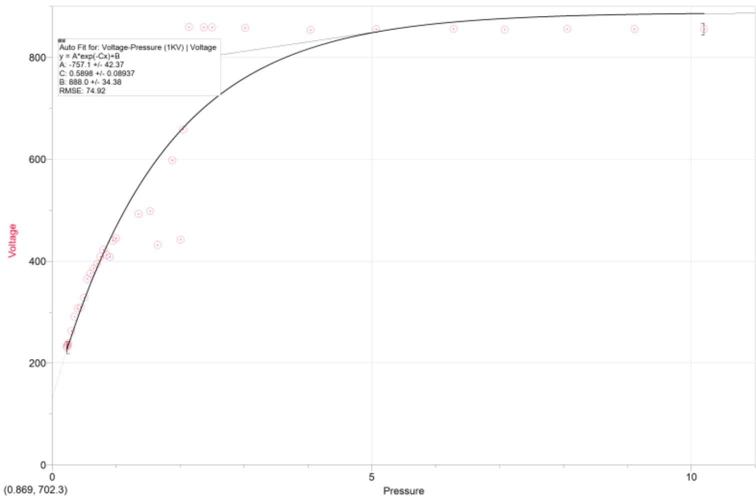

Graph 7: The voltage after the plasma breakdown versus pressure where immediate drop in voltage after plasma breakdown (at 2 mbar) is easily observed.

As a limitation, the power supply was only capable of safely delivering around 6000 volts although rated at 8000 V. The resistor connected in the setup to control the current decreased the amount of voltage in the reactor (the voltmeter was connected so that the potential on the reactor is measured) so only a limited amount of variability in difference of potential was reached, which limited the amount of data points (For plasma to be in star mode, the current needs to be limited). Additionally, reactor was sealed for vacuum efforts however, small leaks might have occurred that can slightly alter the pressure readings.

As a strength, the measurements were all made using devices with electronic output that minimized the chance of random errors occurring. All controlled parameters were kept the same including the temperature and the humidity of the air, also referred to as the fuel.

To conclude, the electrostatic simulation was made with the reactor design parameters to see if a potential well occurs, a key factor in how IEC fusion reactors confine the fuel. After this was confirmed, the Paschen rule was used to see the relation between pressure and plasma breakdown voltages for parallel electrode geometry. The experimental values concurred with those of the Paschen rule with different rates, assumed to be mainly caused by the difference in geometries. As pressure decreased, the plasma breakdown voltage for the reactor also decreased (graph 6). As plasma characteristics in today's fusion reactors are crucial in their operation regarding fusion reactions, this study was hopefully a start that will lead to further analysis regarding the reactor SIEC-K. For future studies involving plasma characteristics, the fusor can be operated in lower pressures with a system capable of altering current in order to deeply grasp plasma operating modes. This would mean the transition between glow-discharge to arc and other plasma modes can be studied with the variable being the current (Graph 3).

Bibliography

(n.d.). Retrieved from http://www.fusor.net/

Arrium. (2016). *Electrical Safety Manual.* OneSteel Whyalla ESN.

Bobkov, V. (2003). *Studies of high voltage breakdown phenomena on.* Munich: Technische Universitat Munchen.

Bölükdemir, A. S. (2013). *DÜŞÜK BASINÇLI EYLEMSİZ ELEKTROSTATİK SIKIŞTIRMALI FÜZYON CİHAZI YAPIMI VE DENEYSEL ÇALIŞMALAR.* Ankara: Gazi Üniversitesi.

Donko, I. K. (2015). *Breakdown in hydrogen and deuterium gases in static and radio-frequency fields.* AIP Publishing LLC.

Eduardo Ramalho, L. R. (2011). BUBBLE DETECTOR'S EVALUATION FOR NEUTRON FIELD EASUREMENTS IN A VERY KNOWN SOURCE. *International Nuclear Atlantic Conference*, (s. 1-15). Brazil.

El-Aragi, G. M. (2017). *Building Inertial Electrostatic Confinement Fusion Device Aimed for a Small Neutron Source.* Cairo: Plasma Physics and Nuclear Fusion Department, Egyptian Atomic Energy.

Elaragi, G. M. (2018). Operation of Inertial Electrostatic Confinement Fusion (IECF) Device Using Different Gases. *Journal of Fusion Energy*, 1-8.

EUROfusion. (2018). https://www.euro-fusion.org/fusion/history-of-fusion/ adresinden alındı

European Nuclear Society. (n.d.). *Fusion*. Retrieved from European Nuclear Society: https://www.euronuclear.org/info/encyclopedia/f/fusion.htm

Farnsworth, P. T. (1966). *US Patent No. US3386883A.*

Gallo, C. F. (1977). *Corona-A Brief Status Report.* Rochester, NY: IEEE.

H. Inga, T. C. (2008). A new Electronic Neutron Dosimeter (END) for reliable personal dosimetry. *The International Society for Optical Engineering*, 1-9.

H.-S. BOSCH, G. H. (1992). IMPROVED FORMULAS FOR FUSION CROSS-SECTIONS AND THERMAL REACTIVITIES. *Nuclear Fusion*, 21.

Hermans, E. (2013). *The Design and Optimization of an Inertial Electrostatic.* Eindhoven: Eindhoven University of Technology.

HyperPhysics. (2000). *Potential: Charged Conducting Sphere*. Retrieved from HyperPhysics: http://hyperphysics.phy-astr.gsu.edu/hbase/electric/potsph.html

Keita Nobe, K. N. (2013). *Study on long time operation of inertial electrostatic confinement fusion (IECF) device.* Tokyo: Tokyo Institute of Technology, Department of Energy Sciences.

Krupakar Murali, G. A. (2010). Effects of chamber pressure variation on the grid temperature in an inertial. *American Institute of Physics*, 1-5.

Linden, T. (2015). Compact Fusion Reactors. *CERN Colloquium* (s. 37). Helsinki Institute of Physics.

MAKO. (2019). *Threaded Needle Valves*. Retrieved from https://mako-products.net/products/mako-products/needle-valves/

Martin, J. E. (2013). *Physics for Radiation Protection.* WILEY-VCH Verlag GmbH & Co. KGaA.

Martins, A. a. (2011). On the propulsive force developed by asymetric capacitors in a vacuum. *Physics Procedia*, 112-119.

Martins, A. A., & Pinherio, M. J. (2011). *On the propulsive force developed by asymmetric capacitors in a vacuum.* Physics Procedia.

Meyer, R. (2006). *Inertial Electrostatic Confinement: Theoratical and Experimental Studies of Spherical Devices.* Columbia: University of Missouri-Columbia.

Miley, H. M. (2001). *Virtual Cathode in a Spherical Inertial Electrostatic Confinement.* Toki, Gifu : National Inst. for Fusion Science.

Murali, G. H. (2014). *Inertial Electrostatic Confinement (IEC) Fusion Fundementals and Applications.* New York: Springer.

Pfeiffer Vacuum. (2013). *The Vacuum Technolgy Book, Vacuum Solutions from a Single Source.* Wuppertal: Pfeiffer Vacuum GmbH.

Pfieffer Vacuum. (2013). *The Vacuum Technolgy Book, Vacuum Measurement, Analysis, Leak Detection.* Wuppertal: Pfieffer Vacuum GmbH.

Pfieffer Vacuum. (2013). *The Vacuum Technology Book, Chambers and Components.* Wuppertal: Pfieffer Vacuum GmbH.

Pfieffer Vacuum. (2013). *The Vacuum Technology Book, Know How Book.* Wuppertal: Pfieffer Vacuum GmbH.

Pfieffer Vacuum. (2013). *The Vacuum Technology Book, Vacuum Generation.* Wuppertal: Pfieffer Vacuum GmbH.

Slichter. (n.d.). Retrieved from What does Standard Deviation Show us About Our Data?: http://science.halleyhosting.com/sci/ibbio/inquiry/standdev2.htm

Smith Pumps. (2019). Retrieved from Explore Smith Pumps: https://www.smithpumps.com/pump-design.php

Taşkolu, H. (2010). *BİR FÜZYON-FİSYON REAKTÖRÜNDE TRISO KAPLAMALI CANDU NÜKLEER YAKIT ATIKLARININ NÖTRONİK ANALİZİ.* Ankara: Gazi Üniversitesi.

Techni Measure. (2016). *Feedthroughs*. Retrieved from https://www.technimeasure.co.uk/feedthroughs/

UCSB Environment Health & Safety Manual. (2007). *Radiation Safety Manual.* California: University of California, Santa Barbara.

University of Oxford. (n.d.). *Fossil Fuels*. Retrieved from Our World in Data: https://ourworldindata.org/

van Limpt, S. (2013). *Characterization of Fusor Jets.* Eindhoven: Eindhoven University of Technology.

Wagenaars, E. (2006). *Plasma breakdown of low-pressure gas discharges.* Eindhoven: Technische Universiteit Eindhoven.

Yiğit, M. (2014). *DÖTERONLA OLUŞTURULAN NÜKLEER REAKSİYONLAR İÇİN AMPİRİK VE YARI-AMPİRİK TESİR KESİTİ FORMÜLLERİNİN ARAŞTIRILMASI.* Ankara: Gazi Üniversitesi.